Near-infrared broadband absorber with film-coupled multilayer nanorods

Xingxing Chen,[1] Hanmo Gong,[1] Shuowei Dai,[1] Ding Zhao,[1] Yuanqing Yang,[1] Qiang Li,[1,3] and Min Qiu[1,2,4]

[1]*State Key Laboratory of Modern Optical Instrumentation, Department of Optical Engineering, Zhejiang University, Hangzhou 310027, China*

[2]*School of Information and Communication Technology, Royal Institute of Technology, Electrum 229, Kista 16440, Sweden*

[3]*e-mail: qiangli@zju.edu.cn*

[4]*e-mail: minqiu@zju.edu.cn*

Received March 8, 2013; revised May 27, 2013; accepted May 28, 2013;
posted May 29, 2013 (Doc. ID 186674); published June 24, 2013

Turning the surfaces of noble metals (metasurfaces) into black (highly absorptive) surfaces can be potentially applied in thermophotovoltaics, sensing, tailoring thermal emissivity, etc. Here we demonstrate an extremely broadband absorber for the 900–1600 nm wavelength range with robust high absorption efficiency. The inexpensive droplet evaporation method is implemented to create patterns of nanoparticles dispersed on a gold film spaced by a thin dielectric layer. The diversity of the complicated random stacking of the chemically synthesized gold nanorods is the major factor for the broad absorption band. Such a metamaterial absorber may pave the way for cost-effective manufacture of large-area black metasurfaces.

OCIS codes: (250.5403) Plasmonics; (310.3915) Metallic, opaque, and absorbing coatings; (240.6680) Surface plasmons; (310.6628) Subwavelength structures, nanostructures.
http://dx.doi.org/10.1364/OL.38.002247

During the past decade, efficient and tunable absorption of metamaterials based on noble metals has been investigated extensively and developed in a variety of branches [1–19]. Efficient absorption is usually enhanced through the excitation of surface plasmon resonances in nanostructured surfaces [5–10]. By tuning the electric and magnetic properties of metamaterial nanostructures through elaborated designs, a number of metasurfaces with high absorption efficiency have been proposed and fabricated using expensive electron-beam lithography or focused-ion-beam milling [2,3,10–15]. By their inherent nature, these fabrication methods hinder mass production and further limit repeatability and applicability. Chemical synthesis, which provides an alternative manufacturing paradigm for large-area high-performance absorbers, is thus put forward and is expected to overcome these limitations. The recent efforts toward manufacturing large-area black metasurfaces are based on either randomly adsorbing chemically synthesized silver nanocubes onto a gold film [16] or depositing Au/SiO_2 nanocomposites [17]. However, only narrowband or visible-range metasurfaces have been experimentally demonstrated [2–6,9–11,13–19] so far, which obviously restricts their potential applications in highly efficient solar cells and sensitive photodetectors. Here we utilize a simple and inexpensive method called droplet evaporation to create a large-area black metasurface with a broad absorption band in the near-infrared region.

As depicted in Fig. 1(a), the whole structure consists of three layers: multiple-layer chemically synthesized gold nanorods randomly deposited on an 80 nm gold film spaced by a 10 nm dielectric layer of aluminum oxide. The scanning electron microscope image of the metasurface is shown in Fig. 1(b). The closely packed gold nanorods form a nonuniform multilayer nanostructure with the number of layers ranging from 2 to 5. Such a multilayer arrangement of gold nanorods will be discussed and verified to be the major contribution to the broadband absorption in this Letter.

In our experiment, the gold nanorods are prepared by using a colloidal seed-mediated, surfactant-assisted growth method adapted from the previous reports [20,21]. The average length and width of the synthesized nanorods are about 60 and 20 nm, respectively. The intrinsic peak absorption wavelength of the nanorods in water is approximately 690 nm, which corresponds to the longitudinal surface plasmon resonance of the nanorods. After the preparation of the gold nanorods in solution, one drop (generally 10 μL) of the dispersion is cast onto the prepared substrate. By controlling the droplet evaporation, multilayer gold nanorods are left on the substrate, and consequently the metasurface is obtained. The fabricated sample is a ring whose diameter is about 2.5 mm and width is about 0.2 mm. This manufacturing method [21] is very simple and cost effective compared with expensive nanofabrication methods such as electron-beam lithography or focused-ion-beam milling.

To measure the transmission (T) and reflection (R) spectra of the absorber, we focus the light beam from

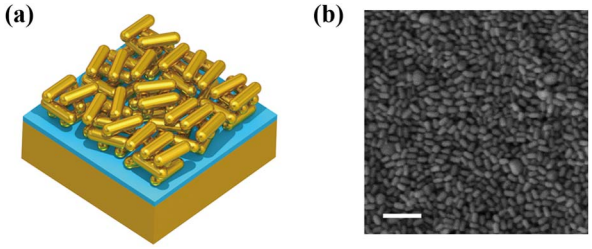

Fig. 1. Morphology of the nanostructure based on multilayer gold nanorods. (a) Schematic diagram of the metasurface consisting of three layers: gold nanorods randomly dispersed on a gold film spaced by a dielectric layer. (b) Scanning electron microscope image of the gold nanorods deposited on the dielectric surface. The scale bar is 200 nm.

a supercontinuum light source through a lens with a focal length of 45 mm and a numerical aperture of 0.3 in normal incidence. The beam spot size on the sample is about 50 μm in diameter, which is much smaller than the patterned area. The incident beam before the sample has a divergence angle of less than 3°; therefore, it has a negligible effect on the absorption spectrum. For the reflection, we utilize another identical lens to couple the light into an optical spectrum analyzer. The transmission can be neglected, considering that the 80 nm gold film's thickness is much larger than the skin depth (about 25–30 nm) of gold [22] in the measured wavelength range. As a result, the absorption (A) is equal to $1 - R$ when considering $T = 0$ in the general formula $A = 1 - R - T$. The absorption spectra for different polarizations are presented in Fig. 2(a). It is obvious that the metasurface is polarization independent because of the random orientations of the gold nanorods. Moreover, it is found that at different spots of the structure, the absorption curves are quite similar, and the absorption efficiency is all very high within a broad band ranging from 900 to 1600 nm [shown in Fig. 2(b)].

To interpret the broadband absorption phenomenon clearly, we also investigate such a metamaterial absorber using the three-dimensional finite element method. Because of the polarization independence of this structure and the shape-based variation of longitudinal collective oscillation of electrons in gold nanorods, only the TE mode in which the electric field is along the long axis of the rods is considered in the simulation, without loss of generality.

Two main factors lead to the highly efficient broadband absorption. One is the size distribution of synthesized gold nanorods. The absorption peak of a single nanorod is generally believed to be strongly dependent on its aspect ratio [23]. Thus the variation in the sizes of the nanorods can broaden the absorption spectrum. However, this effect is really finite, and it could not account for such a broadband absorption. Another factor, the random orientations and stacking of multilayer gold nanorods on the top surface, is assumed to be the major factor. Because of the nonuniform and multilayered properties, different plasmon modes could be excited, such as the fundamental resonance mode of the nanorods and the gap resonance modes between the nanorods. As nanorods are arranged tightly together, these modes interact with each other. As a result, the absorption band is greatly widened. Due to the random and sophisticated distribution of the multilayer gold nanorods, it is impossible to fully illustrate and explain all these interaction mechanisms among the diverse resonance modes. Here several representative configurations as well as their relationships with highly efficient broadband absorption are simulated and analyzed, which provides valuable insight into the broadband absorption.

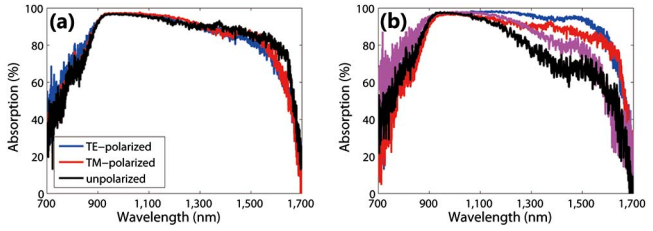

Fig. 2. (a) Absorption spectra for different polarizations of the light: unpolarized (black curve), TE-polarized (blue curve), and TM-polarized (red curve) light. (b) Absorption spectra at different randomly chosen locations of the metasurface.

The situations of multilayer nanorods placed on an 80 nm thick gold film (with dielectric function from the Drude model [24]) spaced by a 10 nm thick aluminum oxide layer (with a refractive index of 1.75) are simulated here. The nanorods are modeled as cylinders with hemispherical end caps. The radius and the length of each nanorod are 10 and 60 nm, respectively. The incident plane wave is polarized along the long axis of the nanorods. Assume that the mismatched distance along the long axis of nanorods between two adjacent layers is d [see the inset in Fig. 3(a)] and that the layer number is N. In Figs. 3(b)–3(g), (d, N) is equal to (5 nm, 2), (3 nm, 3), (7 nm, 3), (6 nm, 4), (10 nm, 4), and (8 nm, 4). With different values of d and N, the peak absorption wavelength of each structure is located at different positions, as displayed in Fig. 3(a). It is found that with the increase of d and N, the absorption peak can be redshifted gradually from 870 to 1420 nm. Without loss of generality, these diverse architectures could be added up to represent a relatively complicated structure to describe the proposed metasurface, though some more complicated crossover issues are not taken into account. Consequently, the superposition of absorption spectra of various substructures gives birth to the highly efficient

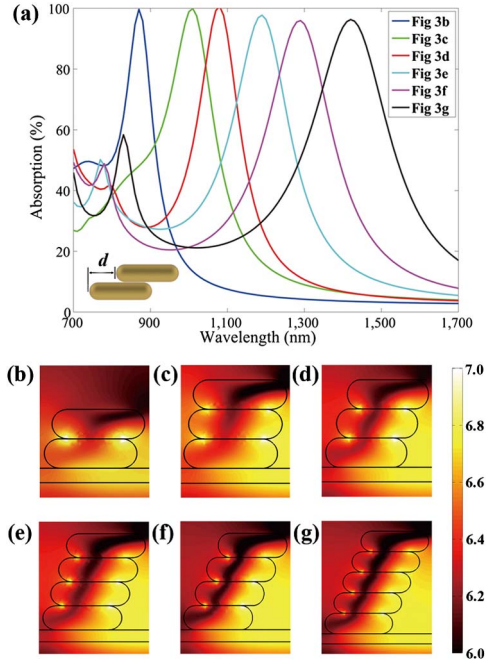

Fig. 3. Simulated absorption spectra and their field distributions. (a) Absorption spectrum of different configurations in (b)–(g), respectively. Inset, schematic diagram of the position of gold nanorods between two adjacent layers. d is the mismatched distance of two neighboring layers. (b)–(g) Distribution of the magnitude of the magnetic field at the peak wavelength of different structures (plot on log scale). The layer number is N; (d, N) is equal to (b) (5 nm, 2), (c) (3 nm, 3), (d) (7 nm, 3), (e) (6 nm, 4), (f) (10 nm, 4), and (g) (8 nm, 5).

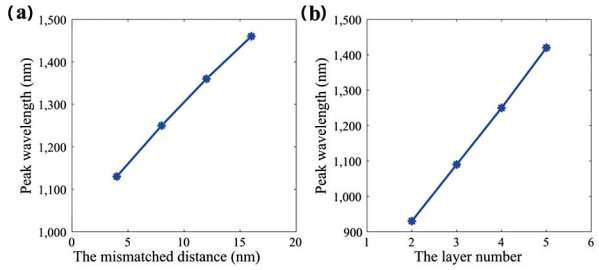

Fig. 4. Peak wavelength versus the mismatched distance and layer number. Peak absorption wavelength (a) as a function of the mismatched distance d at $N = 4$ and (b) as a function of the layer number N at $d = 8$ nm.

broadband absorption spectrum of the whole metamaterial absorber system. In addition, absorption spectra of aggregated nanoparticles on the silica wafer are simulated. It is found that the maximum absorption is only about 40%, which is well below that for the aggregated nanoparticles on the gold film spaced by an alumina layer. Therefore the aggregation on the gold film spaced by an alumina layer is the main factor for the high broadband absorption.

To clarify the effect of d and N on the peak absorption wavelength more clearly, we also investigate the peak absorption wavelength as functions of d and N. Figure 4(a) shows the peak wavelength as a function of the mismatched distance d when layer number N is fixed at 4. The resonant wavelength is linearly redshifted from 1130 to 1460 nm with the increase of d from 4 to 16 nm. A linear relationship between the peak absorption wavelength and the layer number N is also revealed in Fig. 4(b), where d is set to be 8 nm. These results further prove that the diversity of the randomly stacked gold nanorods as well as the multilayer property is the major factor in the highly efficient broadband absorption in the near infrared.

In summary, we have designed, fabricated and characterized a highly efficient absorber with film-coupled multilayer nanorods. Experimental results demonstrate a broadband absorption with high absorption efficiency from 900 to 1600 nm. Moreover, the inexpensive droplet evaporation manufacturing method permits large-area production. Simulations suggest two main contributing factors to the broad absorption band: the dimension dispersions and the diversity of the complicated random stacking of the chemically synthesized gold nanorods, where the latter is the major factor. Such a metasurface may provide possibilities for obtaining large-area light absorbers in applications such as photothermalvoltaics, optical storage, and sensing.

The authors thank Chuangwei Chen and Weidong Shen for their helpful assistances in coating the gold film and dielectric film. This work is supported by the National Natural Science Foundation of China (grants 61275030, 61205030, and 61235007), the Opened Fund of State Key Laboratory of Advanced Optical Communication Systems and Networks, the Fundamental Research Funds for the Central Universities, Doctoral Fund of Ministry of Education of China (grant 20120101120128), the Swedish Foundation for Strategic Research (SSF) and the Swedish Research Council (VR).

References

1. E. Rephaeli and S. H. Fan, Opt. Express **17**, 15145 (2009).
2. N. Liu, M. Mesch, T. Weiss, M. Hentschel, and H. Giessen, Nano Lett. **10**, 2342 (2010).
3. X. L. Liu, T. Tyler, T. Starr, A. F. Starr, N. M. Jokerst, and W. J. Padilla, Phys. Rev. Lett. **107**, 045901 (2011).
4. N. I. Landy, S. Sajuyigbe, J. J. Mock, D. R. Smith, and W. J. Padilla, Phys. Rev. Lett. **100**, 207402 (2008).
5. T. V. Teperik, F. J. Garcia de Abajo, A. G. Borisov, M. Abdelsalam, P. N. Bartlett, Y. Sugawara, and J. J. Baumberg, Nat. Photonics **2**, 299 (2008).
6. E. Popov, D. Maystre, R. C. McPhedran, M. Neviere, M. C. Hutley, and G. H. Derrick, Opt. Express **16**, 6146 (2008).
7. N. Bonod, G. Tayeb, D. Maystre, S. Enoch, and E. Popov, Opt. Express **16**, 15431 (2008).
8. J. S. White, G. Veronis, Z. F. Yu, E. S. Barnard, A. Chandran, S. H. Fan, and M. L. Brongersma, Opt. Lett. **34**, 686 (2009).
9. J. Le Perchec, P. Quemerais, A. Barbara, and T. Lopez-Rios, Phys. Rev. Lett. **100**, 066408 (2008).
10. A. P. Hibbins, W. A. Murray, J. Tyler, S. Wedge, W. L. Barnes, and J. R. Sambles, Phys. Rev. B **74**, 073408 (2006).
11. T. Søndergaard, S. M. Novikov, T. Holmgaard, R. L. Eriksen, J. Beermann, Z. H. Han, K. Pedersen, and S. I. Bozhevolnyi, Nat. Commun. **3**, 969 (2012).
12. X. Chen, Y. T. Chen, M. Yan, and M. Qiu, ACS Nano **6**, 2550 (2012).
13. J. M. Hao, J. Wang, X. L. Liu, W. J. Padilla, L. Zhou, and M. Qiu, Appl. Phys. Lett. **96**, 251104 (2010).
14. K. Aydin, V. E. Ferry, R. M. Briggs, and H. A. Atwater, Nat. Commun. **2**, 517 (2011).
15. M. G. Nielsen, A. Pors, O. Albrektsen, and S. B. Bozhevolnyi, Opt. Express **20**, 13311 (2012).
16. A. Moreau, C. Ciraci, J. J. Mock, R. T. Hill, Q. Wang, B. J. Wiley, A. Chilkoti, and D. R. Smith, Nature **492**, 86 (2012).
17. M. K. Hedayati, M. Javaherirahim, B. Mozooni, R. Abdelaziz, A. Tavassolizadeh, V. S. K. Chakravadhanula, V. Zaporojtchenko, T. Strunkus, F. Faupel, and M. Elbahri, Adv. Mater. **23**, 5410 (2011).
18. Y. H. Su, Y. F. Ke, S. L. Cai, and Q. Y. Yao, Light Sci. Appl. **1**, e14 (2012).
19. J. J. Talghader, A. S. Gawarikar, and R. P. Shea, Light Sci. Appl. **1**, e24 (2012).
20. B. Nikoobakht and M. A. El-Sayed, Chem. Mater. **15**, 1957 (2003).
21. T. Ming, X. S. Kou, H. J. Chen, T. Wang, H. L. Tam, K. W. Cheah, J. Y. Chen, and J. F. Wang, Angew. Chem. Int. Ed. **47**, 9685 (2008).
22. R. Qiang, R. L. Chen, and J. Chen, Int. J. Infrared Millim. Waves **25**, 1263 (2004).
23. W. H. Ni, X. S. Kou, Z. Yang, and J. F. Wang, ACS Nano **2**, 677 (2008).
24. E. D. Palik, *Handbook of Optical Constants of Solids* (Academic, 1985).